Available online at www.sciencedirect.com
SCIENCE DIRECT
Solid State Communications 135 (2005) 574–578
solid state communications
www.elsevier.com/locate/ssc

Impulsive excitation of cyclotron oscillations in a two-dimensional electron gas

J.K. Wahlstrand[a,*], P. Jacobs[a], J.M. Bao[a,1], R. Merlin[a], K.W. West[b], L.N. Pfeiffer[b]

[a]*Department of Physics, The University of Michigan, Ann Arbor, MI 48109-1120, USA*
[b]*Bell Laboratories, Lucent Technologies, Murray Hill, NJ 07974-0636, USA*

Received 16 February 2005; accepted 1 May 2005 by the guest editors
Available online 12 May 2005

Abstract

We report on the impulsive excitation and control of intersubband and hybrid intersubband-cyclotron modes in a two-dimensional electron gas by ultrafast optical pulses. Pump-probe experiments were performed in the reflection geometry on a modulation-doped GaAs/$Al_xGa_{1-x}As$ quantum well at 7 K. Using a pulse shaper to produce multiple excitation pulses, we demonstrate coherent control of charge-density intersubband modes. When a tilted magnetic field is applied, we observe oscillations due to hybrid intersubband-cyclotron modes. The features observed in the pump-probe experiments are consistent in frequency and selection rules with spontaneous Raman scattering data obtained from the same sample.

PACS: 73.21.Fg; 76.40.+b; 42.65.Re

Keywords: D. Cyclotron resonance; E. Inelastic scattering; E. Ultrafast spectroscopy

1. Introduction

After Burstein, Pinczuk, and Buchner first suggested the application of resonant inelastic light scattering to the study of electronic excitations in the two-dimensional electron gas (2DEG) [1], it quickly became an essential tool [2]. Inelastic light scattering compliments infrared spectroscopy in that it is sensitive to excitations of different symmetry. Charge- and spin-density excitations can be distinguished by selection rules, and the wavevector and laser wavelength can be varied to study the dispersion and resonance properties of these excitations. Spontaneous inelastic light scattering has been used to study intersubband spin-density, charge-density, and single particle modes [3], inter-Landau level excitations [4], and collective modes of the fractional quantum Hall liquid [5].

Impulsive stimulated Raman scattering (ISRS) is an ultrafast technique in which an optical pulse of width shorter than the phonon period drives lattice vibrations, leading to coherent phonon oscillations [6]. A similar technique, which might properly be called impulsive stimulated inelastic scattering, analogously drives other low-frequency oscillations, and it was recently used to generate squeezed magnons [7] and entangled spins [8]. In pump-probe experiments, the oscillations are generated by a pump pulse and then sampled by a weaker probe pulse after a time delay τ. The presence of the coherent excitation modifies the optical properties of the system, causing a slight change in the index of refraction. Measuring the intensity or polarization state of the probe pulse as a function of τ produces a signal proportional to the amplitude of the coherent excitation. Furthermore, by shaping the pump pulse, it is possible to excite a particular mode of the system preferentially; this is known as coherent control.

* Corresponding author. Tel.: +1 734 936 0301.
E-mail address: wahlstrj@umich.edu (J.K. Wahlstrand).
[1] Present address: Division of Engineering and Applied Sciences, Harvard University, Cambridge, MA 02138.

0038-1098/$ - see front matter © 2005 Elsevier Ltd. All rights reserved.
doi:10.1016/j.ssc.2005.04.032

Recently, coherent charge- and spin-density oscillations generated this way in a modulation-doped GaAs/$Al_xGa_{1-x}As$ quantum well (QW) were reported [9]. Inelastic scattering by excitations between the ground and first excited conduction subbands is forbidden in a symmetric quantum well. However, when the well is doped on only one side, its reflection symmetry is broken, and these transitions become allowed. In the specific quantum well studied in [9], a set of coherent intersubband excitations was observed. The excitation lowest in energy, the spin-density (SD) mode between the lowest two levels of the quantum well, appears at 2.6 THz. The SD oscillation represents collective motion of the electrons in the quantum well in the growth direction, with electrons of opposite spin oscillating 180° out of phase. At slightly higher energy, 2.9 THz, is the single particle excitation, which is the coherent state of individual electrons in the two lowest subbands. The charge-density (CD) oscillation is shifted higher in energy to 3.3 THz and, similar to the SD, it is a collective motion of the electrons in the growth direction, except that all electrons oscillate in phase. In addition to these ground to first excited state transitions, there is a CD excitation between the first and second excited states, which only appears when electrons have been photoexcited into the first excited state.

Here, we present pump-probe studies of a 2DEG in a doped QW. By using shaped ultrafast pulses, we coherently control the two CD modes. We also performed pump-probe experiments in the presence of a magnetic field which is tilted with respect to the QW growth direction, allowing the excitation of hybrid intersubband-cyclotron oscillations. We discuss the coupling between the cyclotron and CD modes and the possibility of coherently driving other, more exotic excitations which have been previously observed in spontaneous Raman scattering studies.

2. Experiment

The experiments were performed on the same high-mobility modulation-doped single GaAs/$Al_xGa_{1-x}As$ QW as in [9]. The 2DEG was located in a 400 Å thick QW with doping in the barrier on one side. Light entered the sample from the doped side, and passed through a few microns of AlGaAs before interacting with the QW; see Fig. 1. From photoluminescence spectra, we estimate that the Fermi level is 7 meV above the bottom of the conduction band, placing it between the two lowest subbands. This agrees roughly with a self-consistent Poissonian calculation [10], the results of which are shown in Fig. 1(b). Thus, at low temperatures only the ground state of the well is populated.

Spontaneous Raman spectra were obtained using a tunable cw Ti:sapphire laser and Dilor XY spectrometer with the sample at near liquid-He temperatures. The angle between the growth direction and the magnetic field is 45°, and the laser was tuned to 804 nm. In our scattering geometry, the in-plane wavevector was approximately zero.

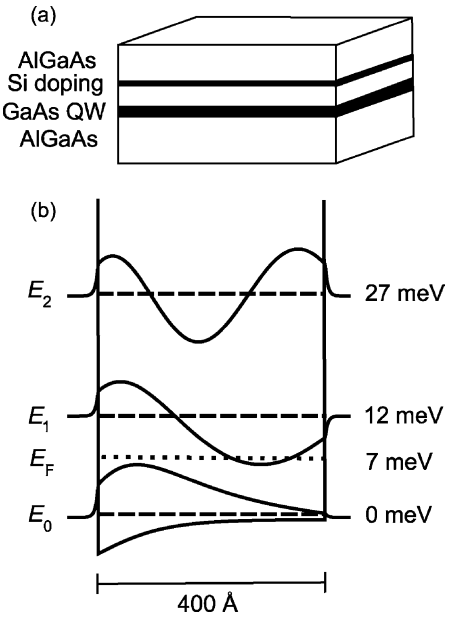

Fig. 1. (a) Sample structure. (b) QW energy diagram and wavefunctions [10].

Spectra were taken with incoming and outgoing polarizations parallel to each other.

Pump-probe experiments were performed in a setup similar to that described in [9]; see Fig. 2. A modelocked Ti:sapphire laser produced 60 fs pulses at a repetition rate of 82 MHz with central wavelength 803 nm. As mentioned earlier, the pump pulse excites the coherent oscillations and a probe pulse follows and samples the oscillations as a function of the time delay between the two pulses. Acousto-optic modulators chopped the pump and probe beams at 3 and 2.95 MHz, respectively, and a lock-in amplifier measured the intensity of the probe pulse at the beat frequency of 50 kHz. In the experiments described here,

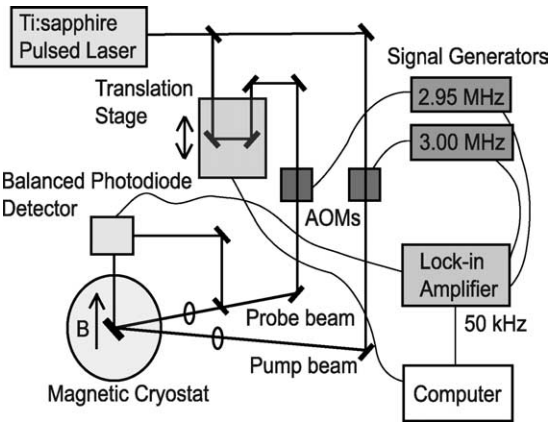

Fig. 2. Pump-probe experimental setup. AOM: acousto-optic modulator.

both beams were linearly polarized and the intensity of the probe pulse was measured, in order to be sensitive only to the CD modes. The spot size on the sample was ~300 μm. The samples were cooled down to 7 K in a cryostat and could be subjected to magnetic fields of up to 6.8 T, produced by a split-coil superconducting magnet.

The pump-probe data was analyzed using discrete Fourier transform and singular value decomposition (linear prediction) [11,12] techniques. Singular value decomposition assumes that the signal is composed of harmonic sinusoids and exponential decays, allowing a least squares fit to the time domain data.

3. Spontaneous Raman scattering

Spontaneous Raman spectra at zero magnetic field are shown in Fig. 3(a). Shown here are the SD (2.6 THz), single particle (2.9 THz), and CD (3.3 THz) modes involving the ground and first excited states of the well [3]. The areal electron density is estimated from the collective mode energies to be $1.9\times10^{11}\,\mathrm{cm}^{-2}$. Not shown is the CD_{12} mode, which appears at higher laser intensity [9]. The bare intersubband transition energies associated with the lowest three subbands are estimated to be $E_{01}=2.9$ THz and $E_{12}=3.8$ THz.

In the presence of a tilted magnetic field, the spectra show peaks associated with hybrid intersubband-cyclotron excitations, depicted in Fig. 3(b). Consistent with previous studies [4,13], we see that the collective modes couple to the cyclotron modes due to the tilted magnetic field. Inter-Landau level inelastic scattering is normally forbidden by selection rules, but in a magnetic field with a component in the QW plane, Landau levels couple to allowed intersubband transitions, leading to hybrid modes which are Raman-active. For a parabolic well, the dispersion of these modes can be calculated analytically [14]. Also appearing with tilted magnetic fields are additional combined resonances which consist of simultaneous intersubband and inter-Landau level excitations [15]. Note the peak at 1 THz, which we tentatively assign to the magnetoroton because of its energy and its appearance at low filling factors.

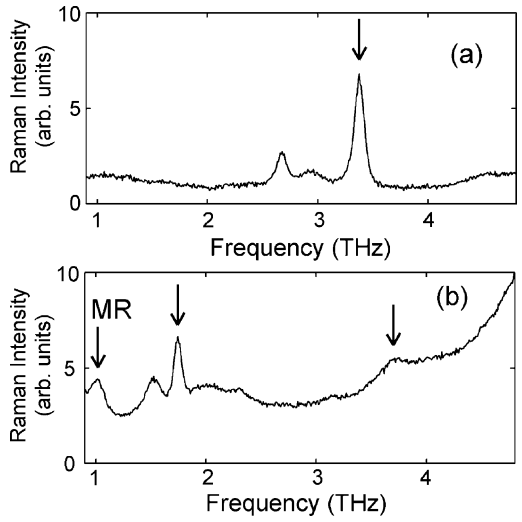

Fig. 3. Spontaneous Raman spectra at (a) 0 T and (b) 6 T. Arrows indicate the CD mode in (a) and the coupled cyclotron-CD modes in (b). The peak labelled MR is tentatively assigned to the magnetoroton.

4. Coherent control of charge-density oscillations

By using multiple pump pulses, it is possible to initiate and then stop the coherent oscillations. This manipulation of the state of the system, known as coherent control, is under investigation as a means to implement gates for quantum information applications [16]. A common way to generate multiple pulses is to use a pulse shaper, which allows one to finely adjust the relative phase and amplitude of the frequency components of the pulse. We used a spatial light modulator consisting of two liquid crystal arrays with 128 pixels each, allowing independent control of the phase and amplitude [17].

As described in Ref. [9], the amplitude of the CD_{12} oscillation depends strongly on the intensity of the pump pulse, because the pump pulse populates the second subband with electrons through photoexcitation. To study this process, we used a pulse shaper to generate two pulses of approximately equal intensity, and varied the time delay T between them. The average power of the pump beam was kept constant as T was varied from 180 to 630 fs. Results are shown in Fig. 4. Pump-probe signals using two pump pulses separated by three different time delays are shown in Fig. 4(a). The pump-probe signal consists of a non-oscillating background, mostly due to photoexcited carriers, and several oscillating signals. The Fourier transform of the fitted signals is shown in Fig. 4(b). Clearly, it is possible to control the relative amplitude of the CD_{01} and CD_{12} modes by varying the time delay between the pump pulses.

In Fig. 4(c), we have plotted the amplitudes of the two modes as a function of T. For independent modes and neglecting damping, we expect the amplitude of each mode to be proportional to $1+\cos\Omega T$, where Ω is the mode frequency. The results for both modes do not exactly fit this function, especially for the CD_{12} mode at small T, indicating that the modes are not independent. This is not unexpected, as both oscillations depend on the population of the second subband. Note that the dependence of the signal on pump-pump time delay could depend on other variables, including the dephasing time of the exciton with which the laser is resonant [18].

5. Hybrid intersubband-cyclotron modes

Pump-probe experiments were also performed in the

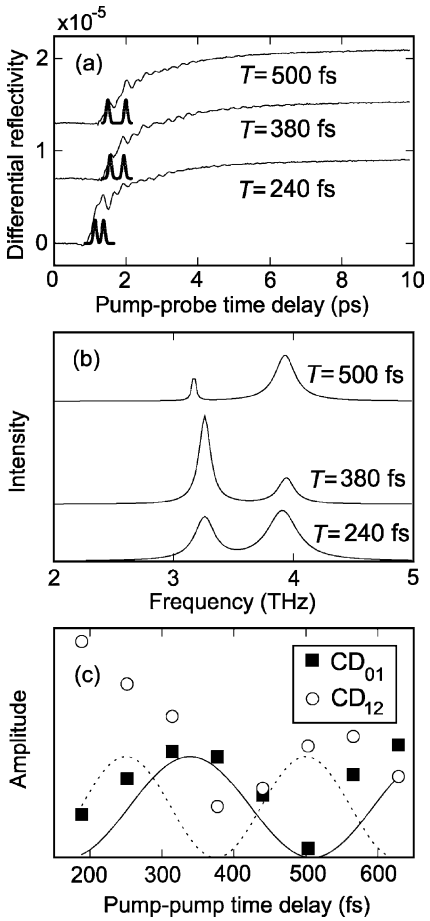

Fig. 4. Coherent control of the CD modes. (a) Pump-probe data. The positions of the two pump pulses are shown. (b) Frequency-domain plot of the Lorentzian fits to the oscillators. (c) Dependence of the CD amplitude on T. Symbols are experimental data: squares represent the CD_{01} mode and circles the CD_{12} mode. The lines show the expected dependence of the CD_{01} (solid) and CD_{12} modes (dotted) based on the model described in the text.

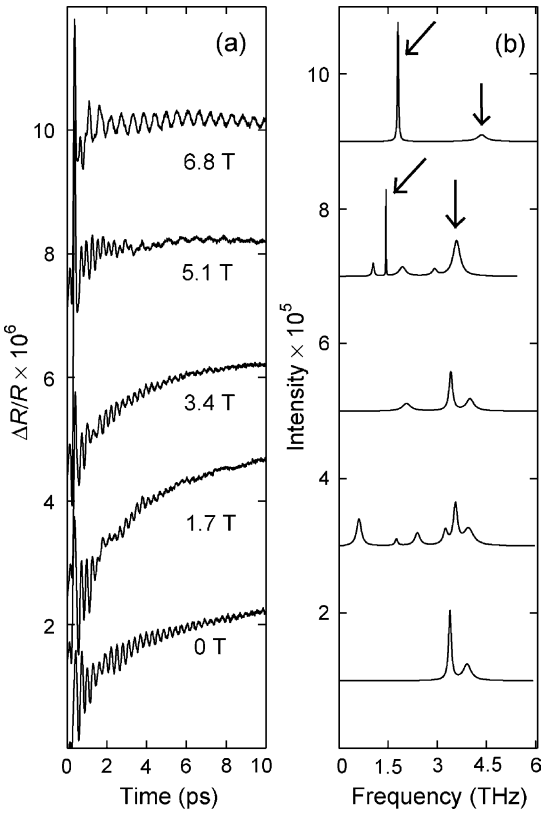

Fig. 5. Results of the pump-probe experiment for various magnetic fields oriented at 45° with respect to the growth direction. (a) The differential reflectivity is plotted as a function of the pump-probe time delay. (b) Singular value decomposition fits to the traces in (a). Arrows indicate the coupled cyclotron-CD modes.

presence of a tilted magnetic field; see Fig. 5. With increasing magnetic field, the CD oscillations are pushed up in frequency, and a low frequency oscillation appears, which we ascribe to the cyclotron mode. At 6.8 T, the data is dominated by this lower-frequency, long-lived oscillation and the much shorter-lived and higher-frequency upper branch, which is mostly an intersubband transition.

The energies of the Raman peaks and pump-probe fits as a function of magnetic field are shown in Fig. 6, together with theoretical curves calculated assuming a parabolic well. These curves follow the coupled cyclotron-intersubband modes. The upper curve differs from the measured Raman peaks because the model neglects many-body effects which push the energy of the CD-like excitations upward from the single particle intersubband energy. The model fits better at higher magnetic fields as the excitations become more cyclotron-like.

In the discussion below and Fig. 6, we follow the convention of Ref. [4] and denote the electron levels as $|n, N\rangle$, where n is the subband index and N is the Landau level index. Thus, the CD excitation between the two lowest subbands (CD_{01}) is the transition $|0,0\rangle \rightarrow |1,0\rangle$. At lower magnetic fields the transition evolves from $|0,0\rangle \rightarrow |1,0\rangle$ to $|0,0\rangle \rightarrow |0,1\rangle$ at higher magnetic fields. The reverse is true for the lower branch. The two dashed lines follow combined resonances that have avoided crossings with the cyclotron and CD modes. These are $|0,0\rangle \rightarrow |1,1\rangle$ for the upper branch and $|0,1\rangle \rightarrow |1,0\rangle$ for the lower. Both branches start from the single-particle excitation frequency, and it can be seen that the lower branch has an avoided crossing near 5 T with the coupled CD-cyclotron modes. The pump-probe results shown in Fig. 6 match the Raman data well. The simultaneous intersubband, inter-Landau level transitions can also be seen. The peak tentatively ascribed to a magnetoroton matches well with the Raman data.

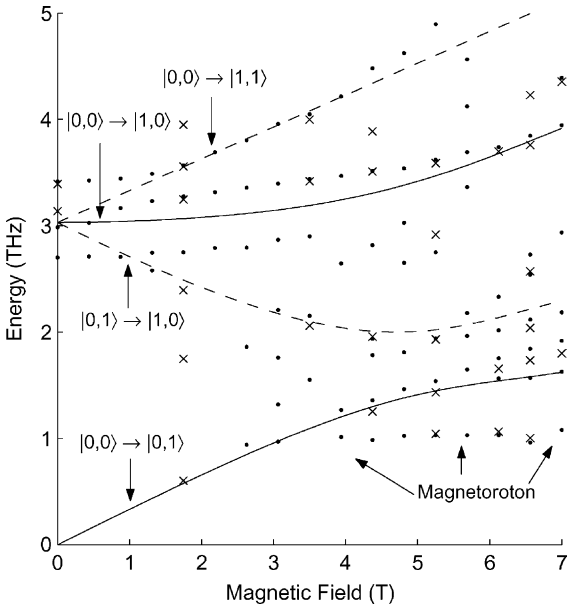

Fig. 6. Frequencies as a function of magnetic field. Dots are Raman peaks and crosses are frequencies obtained from linear prediction fits to the pump-probe data. The solid curves are the magnetic field dependence of the hybrid modes for a parabolic well [14]. The dashed curves are the magnetic field dependence of the combined resonances [15].

6. Conclusion

In summary, we have shown that excitation of coherent cyclotron modes in a 2DEG is possible in the presence of tilted magnetic fields due to coupling between the cyclotron and intersubband modes. This excitation was observed in ultrafast impulsive stimulated inelastic scattering. Also observed were combined resonances involving the cyclotron and intersubband modes. The behavior of the coupled charge-density and cyclotron modes can be fit in the cyclotron-like regions by a parabolic well approximation while, in the CD-dominated regime, many-body effects are important. Also presented here are the results of coherent control using two pump pulses on the CD modes at zero magnetic field, which show a clear dependence on the separation between the two pulses. At higher magnetic fields, this may allow control over the cyclotron excitation coupled to the CD mode.

References

[1] E. Burstein, A. Pinczuk, S. Buchner, Physics of Semiconductors 1978 in: B.L.H. Wilson (Ed.), The Institute of Physics, London, 1979, p. 1231.
[2] G. Abstreiter, R. Merlin, A. Pinczuk, IEEE J. Quantum Electron. QE-22 (1986) 1771.
[3] A. Pinczuk, S. Schmitt-Rink, G. Danan, J.P. Valladares, L.N. Pfeiffer, K.W. West, Phys. Rev. Lett. 63 (1989) 1633.
[4] R. Borroff, R. Merlin, J. Pamulapati, P.K. Bhattacharya, C. Tejedor, Phys. Rev. B 43 (1991) 2081.
[5] A. Pinczuk, B.S. Dennis, L.N. Pfeiffer, K. West, Phys. Rev. Lett. 70 (1993) 3983.
[6] R. Merlin, Solid State Commun. 102 (1997) 207.
[7] J. Zhao, A.V. Bragas, D.J. Lockwood, R. Merlin, Phys. Rev. Lett. 93 (2004) 107203.
[8] J. Bao, A.V. Bragas, J.K. Furdyna, R. Merlin, Nat. Mater. 2 (2003) 175.
[9] J.M. Bao, R. Merlin, K.W. West, L.N. Pfeiffer, Phys. Rev. Lett. 92 (2004) 236601.
[10] Calculated using G.L. Snider's 1D Poisson solver. See I.-H. Tan, G.L. Snider, E.L. Hu, J. Appl. Phys. 68 (1990) 4071.
[11] H. Barkhuijsen, R. de Beer, W.M.M.J. Bovee, D. van Ormondt, J. Magn. Reson. 61 (1985) 465.
[12] F.W. Wise, M.J. Rosker, G.L. Millhauser, C.L. Tang, IEEE J. Quantum Electron. QE-23 (1987) 1116.
[13] G. Brozak, B.V. Shanabrook, D. Gammon, D.S. Katzer, Phys. Rev. B 47 (1993) 9981.
[14] R. Merlin, Solid State Commun. 64 (1987) 99.
[15] V.E. Kirpichev, L.V. Kulik, I.V. Kukushkin, K.v. Klitzing, K. Eberl, W. Wegscheider, Phys. Rev. B 59 (1999) R12751.
[16] X. Li, Y. Wu, D. Steel, D. Gammon, T. Stievater, D. Katzer, D. Park, C. Piermarocchi, L. Sham, Science 301 (2003) 809.
[17] M.A. Wefers, K.A. Nelson, J. Opt. Soc. Am. B 12 (1995) 1343.
[18] A.M. Weiner, J. Opt. Soc. Am. B 11 (1994) 2480.